



HAL
open science

Low Frequency SAS

Fabien Novella, Yan Pailhas, Gilles Le Chenadec, Isabelle Quidu, Michel Legris

► **To cite this version:**

Fabien Novella, Yan Pailhas, Gilles Le Chenadec, Isabelle Quidu, Michel Legris. Low Frequency SAS: Influence of multipaths on Spatial Coherence. 6th Underwater Acoustics Conference & Exhibition, Jun 2021, Virtual meeting, United States. pp.070032, 10.1121/2.0001503 . hal-03519906

HAL Id: hal-03519906

<https://ensta-bretagne.hal.science/hal-03519906>

Submitted on 21 Jan 2022

HAL is a multi-disciplinary open access archive for the deposit and dissemination of scientific research documents, whether they are published or not. The documents may come from teaching and research institutions in France or abroad, or from public or private research centers.

L'archive ouverte pluridisciplinaire **HAL**, est destinée au dépôt et à la diffusion de documents scientifiques de niveau recherche, publiés ou non, émanant des établissements d'enseignement et de recherche français ou étrangers, des laboratoires publics ou privés.



6th Underwater Acoustics Conference & Exhibition

20-25 June 2021

**Underwater Acoustics: Towards Automatic
Target Recognition. Detection, Classification
and Modelling**

Low Frequency SAS: Influence of multipaths on Spatial Coherence

Fabien Novella

*DGA Naval Techniques: DGA Techniques Navales, Brest, 29200, FRANCE;
fabien.novella@ensta-bretagne.org*

Yan Pailhas

*NATO Undersea Research Center: Centre for Maritime Research and Experimentation, Viale San
Bartolomeo 400, 19126 La Spezia, ITALY; yan.pailhas@cmre.nato.int*

Gilles Le Chenadec, Isabelle Quidu and Michel Legris

*Lab-STICC UMR CNRS 6285 ENSTA Bretagne, 2 rue Francois Verny, 29200, FRANCE;
gilles.le_chenadec@ensta-bretagne.fr; isabelle.quidu@ensta-bretagne.fr; michel.legris@ensta-bretagne.fr*

Multipath is an issue for the performance of synthetic aperture sonars. In HF-SAS (high frequency SAS) images, multipaths effects manifest in the hiding of targets, the loss of image contrast and the degradation of interferometry bathymetric estimates and degradation of spatial coherence due to a decrease of the SNR. In this study, the behaviour of a LF-SAS (low frequency SAS) equipped with a full 2D receiving array is analysed. This 2D Rx array enables the observation of the 2D spatial coherence. On the vertical axis, the existence of a multipath reflects on the emergence of lobes in the figure of coherence. Intuitively, the lobes can be understood considering that the direct path and a multipath can be seen from the reception array as two sources that act as a dipole antenna. This study aims at evaluating effects of multipaths on these lobes establishing the link between multipaths and lobes). The study builds upon data acquired by the HRLFSAS designed by NATO CMRE. The effect of multipath is highlighted thanks analytical modelisation and a comparison between observed coherence and the one predicted from application of the Van Cittert Zernike theorem to the distribution of energy estimated by a vertical beamforming.

INTRODUCTION

The notion of coherence is defined by Goodman as the ability of light beams to interfere.¹ Thus two types of coherence can be defined: temporal coherence and spatial coherence. Temporal coherence refers to the ability of a waveform to interfere with a delayed version of itself at a same point. Spatial coherence refers to the ability of a waveform to interfere with a spatially shifted but not delayed version of itself. Mutual coherence refers to the addition of these two components. In the field of Synthetic Aperture Sonars (SAS) both spatial and temporal coherence of the backscattered acoustic field are exploited. In order to coherently sum multiple looks of a scene to form the SAS image, the sonar has to be positioned with accuracy better than a fraction of a wavelength.² A classical way to deal with this issue is the Displace Phase Center (DPC) motion estimation technique.³ This technique consists in estimating the coherence between transducers during successive pings and therefore different antenna positions. The maximum coherence detection then allows to estimate the displacement of the antenna during these different pings. The estimation of bathymetry is based on the measurement of the phase difference between the images obtained by vertically separated antennas. It has been shown that there is a distance beyond which the difference between the two antennas is too large and the loss of spatial coherence between the measurements results in too much noise in the interferogram.⁴ In addition, the edges of manufactured objects are known to offer a greater length of coherence than the background on which they are placed: they are called permanent scatterers. This property is used for the detection of manufactured objects and their segmentation from the background.⁵

Thus, spatial coherence is an important notion in SAS processing. The understanding and the quality of the modelling of this phenomenon are therefore essential. In this paper, we focus on the influence of multipaths on spatial coherence. After theoretical reminders on spatial coherence and its estimation, multipaths existing in data from the TORHEX'18 campaign conducted by CMRE with the HRLFSAS sonar are identified thanks to a high-resolution beamforming. Finally, the influence of multipaths is highlighted by an analytical model comparing the observed coherence with that predicted by the Van Cittert Zernike (VCZ) theorem from the energy distribution estimated by beamforming.

1. SPATIAL COHERENCE: THEORETICAL ASPECTS

A. FUNDAMENTALS OF COHERENCE AND THE VAN CITTERT ZERNIKE THEOREM (VCZ)

Van Cittert Zernike's theorem was developed in the framework of statistical optics. The basis of this theorem was laid by Van Cittert in 1934⁶ and then developed by Zernike in 1938⁷ in order to write down the interference fringes observed in the Young's slit experiment. The resulting theorem relates the coherence of a radiated field measured at two points in space to the intensity distribution of an incoherent source. The theorem can be formulated as follows:¹

“Spatial coherence is proportional to the 2D Fourier transform of the energy distribution across the source”

The notion of an incoherent source on which the VCZ theorem is based should be questioned. Indeed, this notion may seem irrelevant in the pulsed ultrasound framework. For this purpose Mallart and Fink consider a source insonifying an incoherent scattering medium.⁸ A pressure field is then backscattered towards a receiver. At each instant, the backscattered field comes from a finite volume of the scattering medium named isochronous volume. Thus it is possible to consider that the backscattered acoustic field is produced by a volume source which would occupy the whole isochronous volume. This source will be called the equivalent source in the following. Insofar as the isochronous volume has a large number of scattering elements and that these are randomly distributed within this volume, the equivalent source can be considered

as incoherent. In the remainder of this study, the insonified volume of the background is considered as an incoherent equivalent source to which the VCZ theorem will be applied.

B. PRACTICAL ESTIMATION OF THE SPATIAL COHERENCE

Spatial coherence between two zero-mean signals s_1 and s_2 acquired at two distinct points P_1 and P_2 is usually evaluated through the mutual coherence $J(P_1, P_2)$ and the factor of coherence $\gamma(P_1, P_2)$ with:

$$J(P_1, P_2) = \Gamma(P_1, P_2)|_{\tau=0} \quad \text{and}, \quad (1)$$

$$\gamma(P_1, P_2) = \frac{J(P_1, P_2)}{\sqrt{(J(P_1, P_1) \cdot J(P_2, P_2))}} \quad (2)$$

where $\Gamma(P_1, P_2)|_{\tau=0}$ is the intercorrelation between signals s_1 and s_2 evaluated at 0 temporal lag. Let us consider a sonar formed by one transmitter and four receivers lying in the same plane (see Fig. 1 (a)). A possible coherence as function of distance between receivers is represented in figure 1 (b).

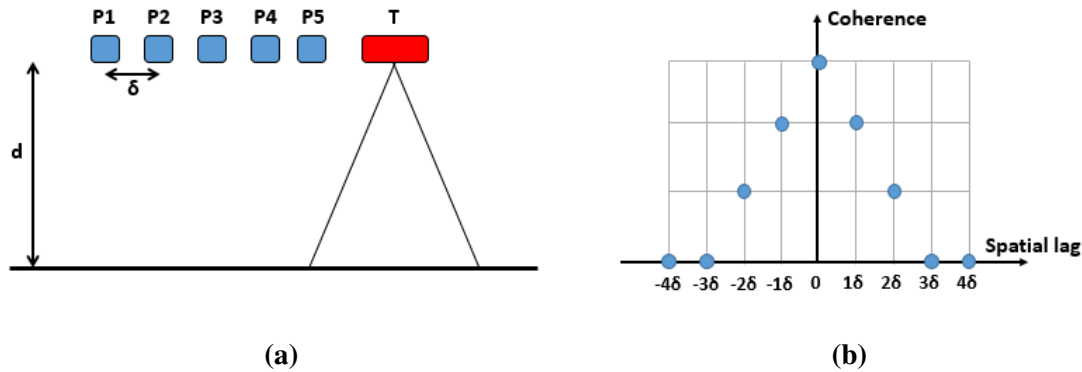


Figure 1: (a) A one dimensional array with equally spaced hydrophones. δ is distance between hydrophones and d is depth - (b) Typical coherence function for such an array.

Practical computation of the coherence function is presented here. Positions P_1 and P_2 in Eq. (1) and (2) refer to the locations of receiver elements. Mutual coherence can thus be computed for each pairs of receivers by intercorrelation between signals (see Eq. (1)). Then mutual coherence is normalized by autocorrelations of both signals to compute the degree of coherence (see Eq. (2)). Finally mutual coherences are grouped by element separation and averaged in order to compute the degree of coherence for a given spatial lag. Therefore, for a spatial lag μ , the entire calculation is summarised by the following expression:

$$\hat{\gamma}(\mu) = \frac{1}{N_\mu} \sum_{N_\mu} \frac{\langle s_i(t) \cdot s_j^*(t) \rangle_t}{\sqrt{\langle s_i^2(t) \rangle_t \cdot \langle s_j^2(t) \rangle_t}}, \quad (3)$$

where N_μ is the number of receiver pairs that are separated by a distance μ .

C. HRLFSAS AND 2D SPATIAL COHERENCE

The system studied in this paper is the HRLFSAS sonar developed by NATO CMRE.^{9,10} It consists of a 2D wideband low frequency transmit antenna that insonifies a seafloor. The receive antenna is also 2D and thus provides observation of spatial coherence both in the horizontal direction (along track) and in the

vertical direction (across track). A previous study has already investigated the coherence of this system in the horizontal direction and showed a good match between the observed coherence and that predicted by the VCZ theorem.¹¹ In this paper we will focus on coherence in the vertical direction. As an illustration, Fig. 2 shows the 2D spatial coherence calculated over 4 different time windows corresponding at following range intervals (in meters): [23.1, 29.4], [35.6, 41.8], [43.7, 50.0] and [52.5, 58.8]. The dx axis of the coherence figure corresponds to the vertical direction and the dy axis to the horizontal direction. It can be seen that in the vertical direction, lobes appear and disappear depending on the time window studied. In the rest of this paper, we try to explain the appearance and position of these lobes by the presence of multipaths.

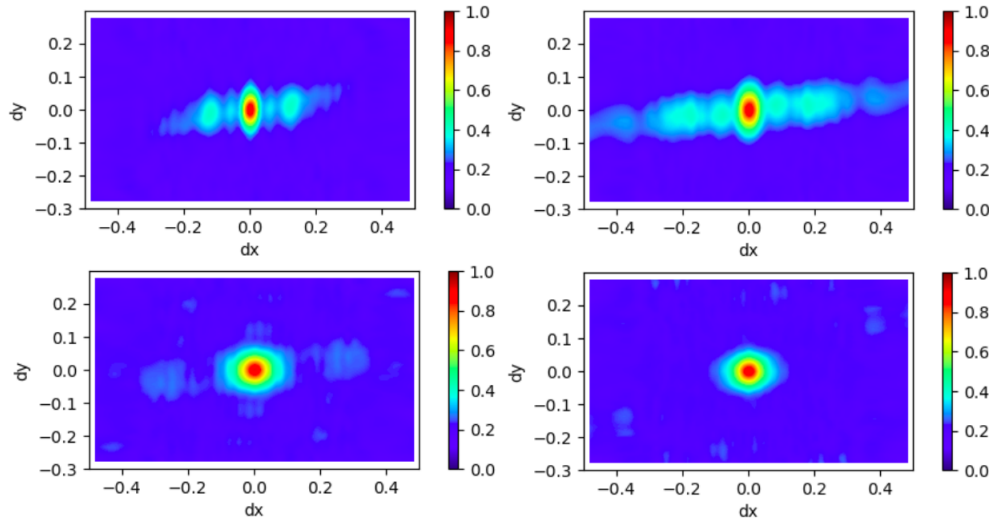


Figure 2: 2D spatial coherence calculated over 4 different time windows

2. INFLUENCE OF MULTIPATHS ON SPATIAL COHERENCE

Multipaths in SAS sonar is a widely studied notion and it is known that multiple reflections via the sea surface can affect the performance of sonar with several effects:

- Can potentially lower the temporal coherence between pings and so decrease the accuracy of micronavigation necessary for image focusing.¹²
- Can reduce spatial coherence in interferometry and so affect the ability of SAS to compute an accurate bathymetric map
- Can add unwanted signals to the SAS image and so decrease contrast between shadows and strong reflections that make Automatic Target Recognition (ATR) algorithms less efficient.

A. A FIRST ANALYTICAL APPROACH

In order to gain insight into the effect of the presence of a multipath in the received signals on the vertical coherence, we can model the energy distribution in the vertical plane as the sum of two Gaussian distributions of the same aperture σ and centred on two different arrival directions ϕ_1 and ϕ_2 .

$$s(\phi) = e^{-\frac{(\phi-\phi_1)^2}{2\sigma^2}} + e^{-\frac{(\phi-\phi_2)^2}{2\sigma^2}} \quad (4)$$

According to the Van Cittert Zernike theorem (see Sec. 1.A), spatial coherence is proportional to the Fourier transform of the distribution of energy $s(\phi)$

$$\begin{aligned}\gamma &= \int_{-\infty}^{+\infty} s(\phi) e^{-j\omega\phi} d\phi \\ &= 2\sigma\sqrt{2\pi} e^{-\frac{\omega^2\sigma^2}{2}} \cos\left(\frac{\Delta\phi \cdot \omega}{2}\right) \quad \text{with} \quad \Delta\phi = \phi_2 - \phi_1\end{aligned}\quad (5)$$

If the proportionality factors in equation 2 are not taken into account, there remains in this equation an exponential term which corresponds to the Fourier transform of a Gaussian, i.e. of the coherence which would have been induced by only one of the two sources modulated by a cosine which induces oscillations. The frequency of the oscillations depends only on the difference in the directions of arrival. Equation (5) can thus be interpreted as follows: in the presence of multipath, the observed coherence corresponds to the coherence that would have been observed in the absence of multipath modulated by oscillations whose frequency depends on the difference in arrival angles. The greater the difference in arrival directions, the faster the frequency of the oscillations. This point is illustrated in Fig. 3, which shows the associated coherence figure for two different arrival directions. For a $\Delta\mu = 17$, three peaks are observed whereas for $\Delta\mu = 34$ six peaks are observed in the same coherence length.

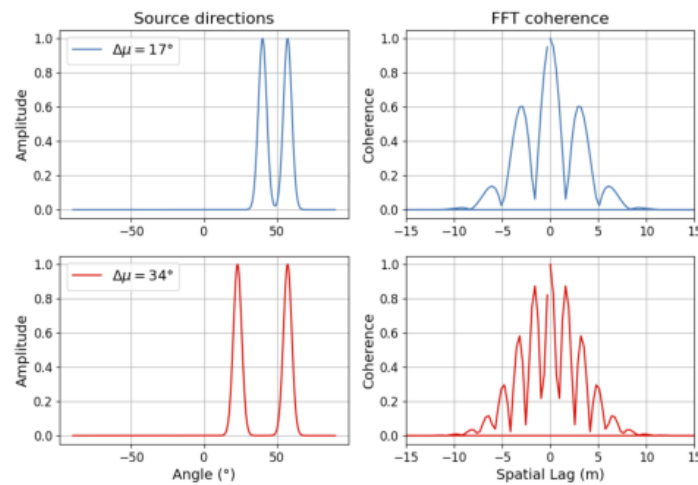


Figure 3: (left) Distributions of energy - (right) Coherences estimated through VCZ theorem

This analysis shows that the presence of a multipath that behaves as a second source in the energy distribution spectrum received by a receiving antenna induces oscillations in the coherence pattern. However, these oscillations cannot always be observed. This is because the transducers of a receiving antenna are not point-like and are therefore necessarily spaced at a distance of at least a few centimetres. We have shown that the speed of oscillation depends on the difference in the angles of arrival. Thus for a large difference, the oscillations are very fast and if their period is less than the inter-sensor distance, then they cannot be observed.

B. MULTIPATHS IDENTIFICATION

In order to study the influence of the presence of multipath on the coherence pattern, we start in this section by trying to observe the multipaths existing in the signals acquired during the tests. We will only be interested in the first two orders, i.e.:

- First order multipath (in blue on figure 4): refers to the wave that would have been scattered and then reflected specularly on the surface before reaching the receiving antenna or conversely, the wave reflected specularly on the surface and then backscattered towards the receiving antenna,
- Second order multipath (in red on figure 4): refers to the wave that would have been specularly reflected on the bottom, then on the surface, and finally backscattered on the bottom towards the antenna or conversely, the wave scattered on the bottom towards the surface and then specularly reflected on the surface and on the bottom to the receive antenna.

These multipaths are illustrated on figure 4.

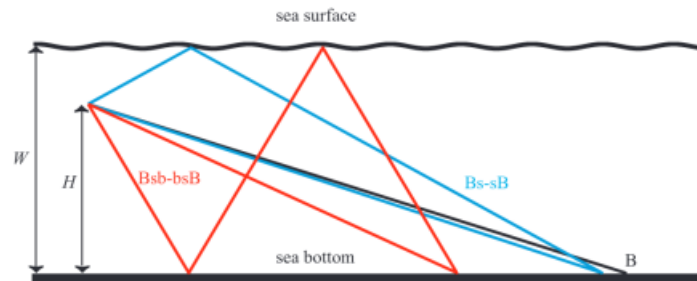


Figure 4: First and second order multipaths from bottom backscatter.¹³

Classical time and delay beamforming does not allow us to obtain a resolution small enough to distinguish direct path and multipaths. To deal with this issue, a high resolution beamforming algorithm can be used. The MUSIC algorithm is an adaptive method based on an eigen decomposition of the correlation matrix estimate. The measurement space is then divided into two subspaces: the signal space according to the main eigenvalues of the decomposition and the noise space according to the others.¹⁴ The length of the signal space corresponds to the number of sources expected. For this study, two sources are expected at the beginning of the signal and three later. Assuming that the signal subspace is orthogonal to the noise subspace, the angular pseudo-spectrum can be computed. Locations of each peaks on the pseudo spectrum correspond to the arrival direction of each source. However it is known that the magnitude of the peak does not correspond to the intensity of the target. For our application, we are interested on distribution of energy i.e. on both the direction and the intensity of sources. Directions are estimated thanks to the MUSIC algorithm so the problem then reduces to the estimation of the signal powers from each of the identified directions. Source intensities can be reconstructed using information contained on the covariance matrix of data and assuming uncorrelated signal from different directions, which is usually the case between multi and direct paths.¹⁵

Results of the beamforming in the vertical plane is presented on Fig. 5. The presence of the bottom echo, a first-order multipath from the surface and a second-order multipath from the bottom arriving later can be noticed. The presence of the bottom echo, a first-order multipath from the surface and a second-order multipath from the bottom arriving later can be noticed. At low ranges, a second contribution is also noticed, coming from a slightly different direction than the one at the bottom. In view of the direction of arrival (about 30°), this contribution is probably due to a buried reflection. This contribution is designated as “volume” in Fig. 5.

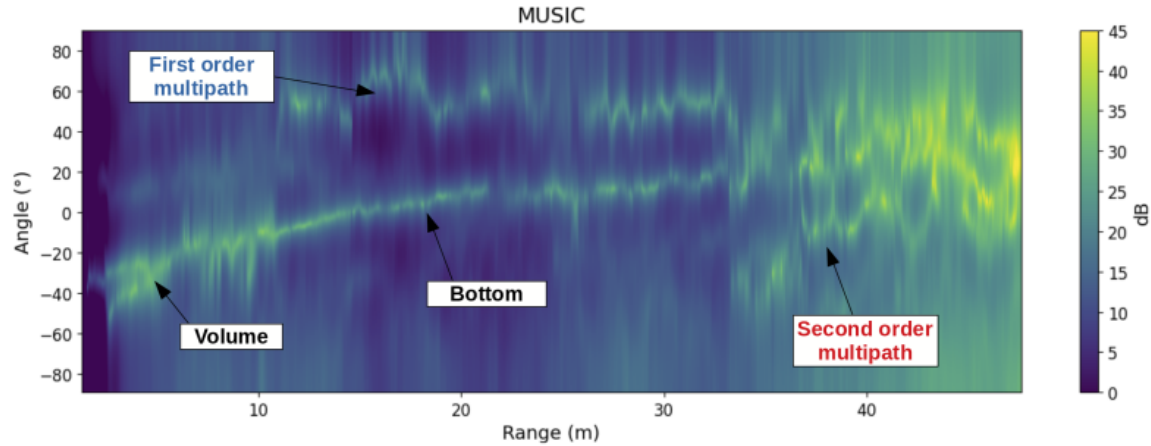


Figure 5: High resolution vertical beamforming and multipaths identification

C. OBSERVED COHERENCE

We saw in Sec. 2.A that the frequency of the oscillations depended on the difference in arrival directions and that if this difference was too great, the inter-sensor spacing made it impossible to observe the oscillations. We therefore carried out the study on a time window located at the beginning of the range where the buried contribution arrives in a direction very close to that of the bottom. In this time window the first order multipath contribution from the surface is also present. This temporal window is illustrated in red on Fig. 6.b. On Fig. 6.a, the degree of coherence in the vertical direction, computed on this temporal windows, is plotted.

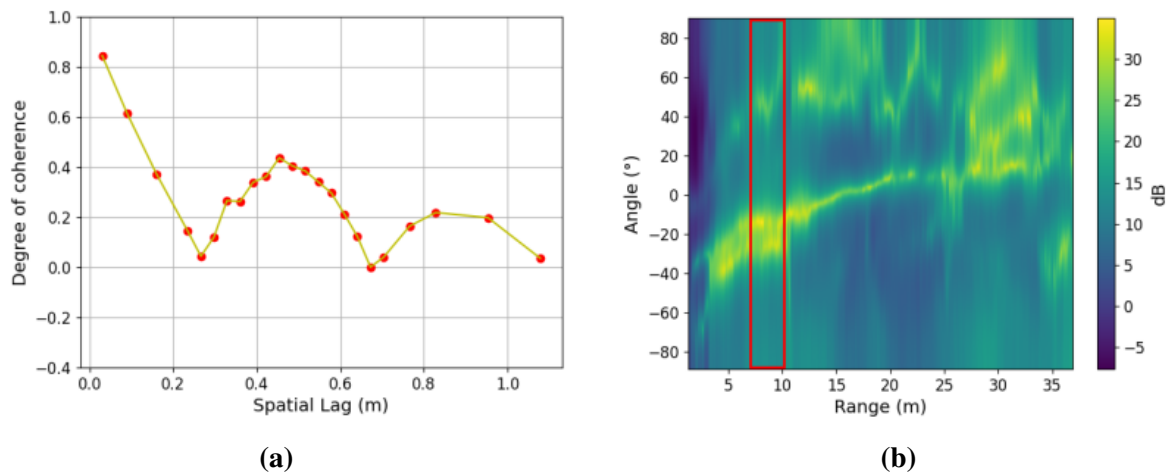


Figure 6: (a) Degree of coherence on the vertical direction - (b) Temporal windows used

D. VCZ COHERENCE

As it is explained in Sec. 1.A, spatial coherence can be predicted thanks to the VCZ theorem through the Fourier transform of the distribution of energy across the source. The mean distribution of energy is estimated by averaging the result of the beamforming on the temporal window. Fig. 7.a is the distribution of energy over the whole temporal window and Fig. 7.b is the mean distribution of energy. In Fig. 7.b, one can notice a first peak at nearly 50° that corresponds to a multipath coming from surface, the higher

peaks at -20° corresponds to the bottom contribution and the other one at -25° corresponds to the buried contribution.

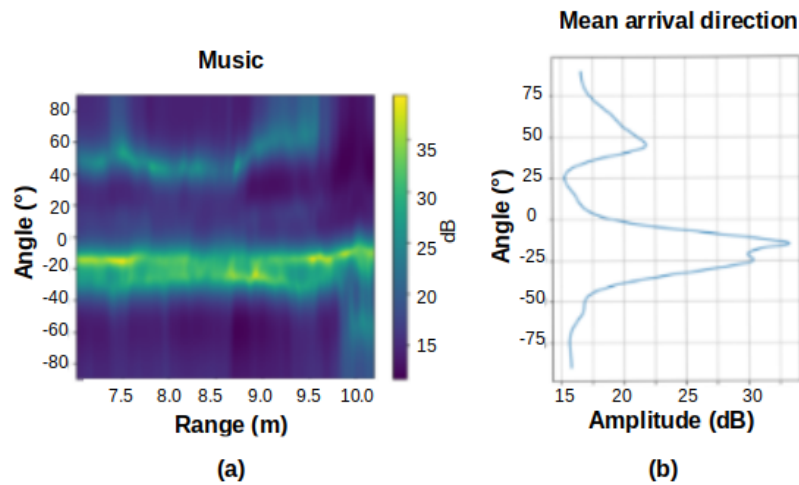


Figure 7: (a) Distribution of energy over the temporal window - (b) Mean distribution of energy

According to the VCZ theorem, spatial coherence can be predicted by taking the Fourier transform of this mean distribution of energy. Strictly speaking, in order to estimate coherence as a function of spatial displacement, the VCZ theorem should be applied on a distribution of energy versus vertical offset and not as function of vertical tilt angle. However with such a distribution, the travelled distance is different for each multipath and so the influence of a multipath that would be observed, would not be the expected one. However, VCZ can be applied on the angular distribution of energy using far field assumption (complied with for this study). Indeed, under this assumption, plane wavefronts reach the receiving antenna and spatial frequency on the antenna is equivalent to arrival direction. That is illustrated in Fig. 8 (blue curve). In this figure, this predicted coherence is compared to the one observed on Sec. 2.C. A good agreement can be noticed between observed and predicted coherences. The major difference is at zero spatial lag. That can be explained by the fact that the predicted coherence is normalised to one whereas the observed one is decreased by the signal to noise ratio.

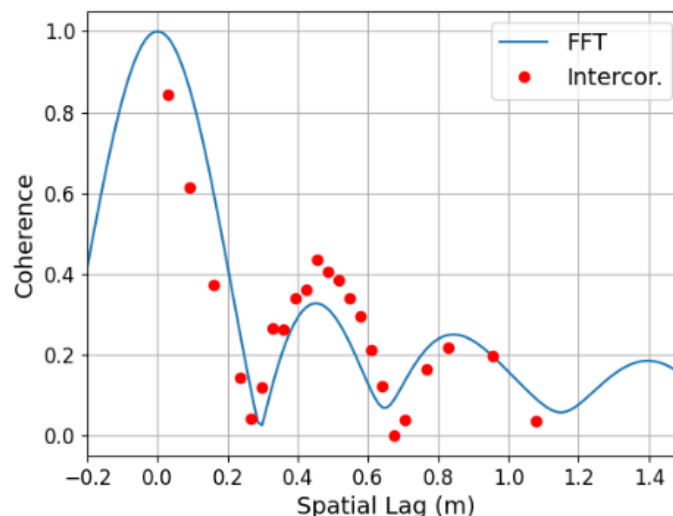


Figure 8: Comparison between coherence observed (red dots) and predicted by the VCZ theorem (blue curve)

CONCLUSION AND FUTURE WORKS

To conclude, it has been shown that multipaths affects vertical coherence by adding oscillations on the figure of coherence. That has been observed on real data and by applying the VCZ theorem to an analytical model and to the mean distribution of energy estimated by an high resolution beamforming. Comparison between these coherences shows good agreement and tends to illustrate the influence of multipath on the coherence figure. The study shows that in the presence of a multipath, oscillations appear on the coherence pattern and the frequency of the oscillations depends on the difference in arrival directions: the greater the difference in arrival directions, the higher the frequency of oscillation. Finally, in order to go further in the understanding of this phenomenon, we plan to develop an analytical model of coherence suitable for SAS configuration.

ACKNOWLEDGEMENTS

This work is conducted as part of a PhD funded the French Defence Agency. We also want to thanks NATO CMRE for the availability of the TORHEX'18 dataset.

REFERENCES

- ¹ Joseph W Goodman. Statistical optics. *New York, Wiley-Interscience, 1985, 567 p.*, 1, 1985.
- ² Roy Edgar Hansen. Introduction to synthetic aperture sonar. In N. Z. Kolev, editor, *Sonar Systems*, chapter 1. IntechOpen, Rijeka, 2011.
- ³ A. Bellettini and M. A. Pinto. Theoretical accuracy of synthetic aperture sonar micronavigation using a displaced phase-center antenna. *IEEE Journal of Oceanic Engineering*, 27(4):780–789, 2002.
- ⁴ Torstein Saebo. Seafloor depth estimation by means of interferometric synthetic aperture sonar. 01 2010.
- ⁵ Y. Pailhas, C. Capus, and K. Brown. Permanent scatterers detection using raw SAS data. *Proceedings of Meetings on Acoustics*, 17, 01 2012.
- ⁶ P.H van Cittert. Die wahrscheinliche schwingungsverteilung in einer von einer lichtquelle direkt oder mittels einer linse beleuchteten ebene. *Physica*, 1(1):201 – 210, 1934.
- ⁷ F. Zernike. The concept of degree of coherence and its application to optical problems. *Physica*, 5(8):785 – 795, 1938.
- ⁸ Raoul Mallart and Mathias Fink. The van cittert–zernike theorem in pulse echo measurements. *The Journal of the Acoustical Society of America*, 90(5):2718–2727, 1991.
- ⁹ A. Xenaki and Y. Pailhas. Compressive synthetic aperture sonar imaging with distributed optimization. *The Journal of the Acoustical Society of America*, 146(3):1839–1850, 2019.
- ¹⁰ Y. Pailhas, S. Fioravanti, F. Aglietti, A. Carta, A. Sapienza, and D. Galletti. Low frequency SAS 2D transmitter array calibration. In *OCEANS 2019 - Marseille*, pages 1–6, 2019.
- ¹¹ Fabien Novella, Yan Pailhas, Isabelle Quidu, and Gilles Le Chenadec. Low frequency sas: Spatial coherence study. *Proceedings of Meetings on Acoustics*, 40(1):070016, 2020.

- ¹² L. Wang, G. Davies, A. Bellettini, and M. Pinto. *Multipath Effect on DPCA Micronavigation of a Synthetic Aperture Sonar*, pages 465–472. Springer Netherlands, Dordrecht, 2002.
- ¹³ A. Bellettini, M. Pinto, and L. Wang. Effect of multipath on synthetic aperture sonar. In *WCU Paris 2003*, 2003.
- ¹⁴ K.W. Lo. Adaptive array processing for wide-band active sonars. *IEEE Journal of Oceanic Engineering*, 29(3):837–846, 2004.
- ¹⁵ Lardies Joseph, Hua Ma, and Marc Berthillier. Power estimation of acoustic sources by sensor array processing. *Open Journal of Acoustics*, 03:1–7, 01 2013.